Effect of dry density on the relationship between water content and TDR-measured apparent dielectric permittivity in compacted clay

A. Pozzato & A.Tarantino
Dipartimento di Ingegneria Meccanica e Strutturale, Università degli Studi di Trento, Italy

J. McCartney & J. Zornberg
University of Texas at Austin, Austin, TX, United States

ABSTRACT: The paper presents an experimental investigation of the effect of dry density on dielectric apparent permittivity. It was observed that the effect was not significant, but not negligible for sensitive applications. It is shown that the effect of dry density can be successfully modeled using a three-phase 'refractive index' model. It is also shown that Topp's equation can accurately predict water content provided bulk electrical conductivity is accounted for.

1 INTRODUCTION

The volumetric water content, θ_V, is a key variable in unsaturated soil mechanics and needs to be measured both in the laboratory and the field. Time domain reflectometry (TDR) is a technique that can be successfully used for this purpose. This technique is based on the measurement of the dielectric permittivity of the soil, K_a, which is in turn related to the volumetric water content through a suitable calibration curve. An empirical calibration curve was presented by Topp et al. (1980) suggesting a unique relationship between K_a and θ_V. However this curve was developed for agriculture soils which have dry densities typically lower than compacted soils used in geotechnical engineering. The purpose of this study is to investigate the effects of dry density on the K_a - θ_V relationship.

2 MATERIAL AND SPECIMEN PREPARATION

A low plasticity compacted clay (RMA soil) was selected for use in investigating the impact of density on the TDR calibration. The soil has a plastic limit w_P=0.12, liquid limit w_L=0.27 and hygroscopic water content w_H=0.02. The grain size distribution showed it to have 0.24 clay fraction, 0.36 silt fraction, and 0.4 sand. The specific gravity of the soil is 2.71, and the saturated hydraulic conductivity is about $5*10^{-6}$ m/sec. The maximum dry density, ρ_d, obtained using the standard Proctor compaction effort is 1.9 g/cm^3, and the optimum water content, w_C was 12.9% (McCartney 2007).

To prepare the samples for calibration, dry soil was placed in a motorized mixer and sprayed with a predetermined amount of demineralised water while continuously mixing the soil. Samples were prepared at water contents ranging from 9.7% to 17.7%. The moistened soil was stored for at least two days to allow moisture equilibration.

A PVC mold having a diameter of 103 mm was used to compact the soil. The soil was compacted in six layers 19.4 mm thick using a drop hammer to obtain specimen 116.4 mm high. Each layer was compacted which a same target dry density.

Three series of samples were prepared, each with a different dry density. The dry densities and the gravimetric water content of the samples used in the TDR measurements are shown in Figure 1.
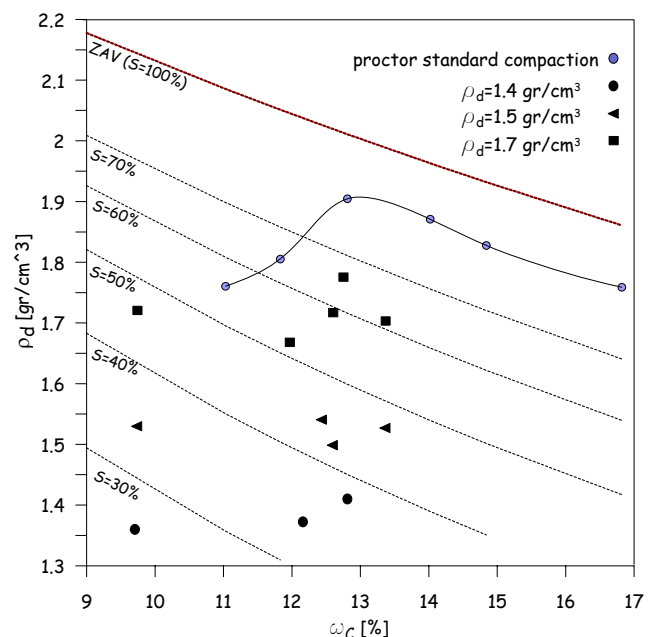

Figure 1. Samples prepared for TDR calibration (the standard Proctor compaction curve is shown for reference)

3 EXPERIMENTAL PROCEDURE

3.1 *Instrumentation*

The TDR system used in this study consists of an electromagnetic step pulse generator with a fast rise time, a time equivalent sampling oscilloscope, and a trifilar waveguide. A commercially available TDR system was used in this study (MiniTrase). The oscilloscope and the step pulse generator were incorporated into the MiniTrase (6050X3) and the waveforms were collected via serial port with the TraseTerm software. An uncoated, 8-cm buriable probe (Model 6111, Soil Moisture Equipment Corp., Santa Barbara, CA) was used in this study. The probe had three 3mm stainless steel rods having spacing, *s*, of 12.5mm. A 3 m of low-loss RG-58 coaxial cable was used.

3.2 *TDR installations*

Three types of measurements were performed; measurements in demineralised water and air, in layers of water and air, and in compacted soil. For measurement in soil, the TDR probe was inserted centrally into the cylindrical specimen still in the mould (Figure 2). For measurement in water and in layers of air and water, the probe was inserted centrally in a container of the same size as the mould. The measurements were performed in a temperature-controlled laboratory (22 ±1°C).
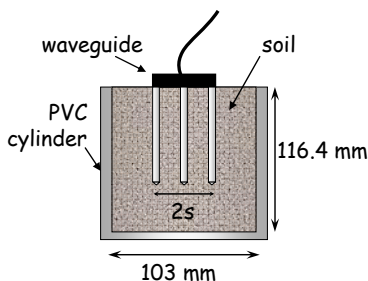

Figure 2. Probe installation in the compacted soil

3.3 *TDR measurement*

A typical reflection waveform with a large time window, obtained from measurement in water, is shown in Figure 3.

At *t=2ns*, the voltage step pulse launched into the transmission line is recorded by the oscilloscope. The oscillations following the rising step are perhaps aberrations due to the internal circuit and reflection from the front panel. The signal becomes stable while travelling down the cable.

At *t=15ns*, a drop in voltage amplitude is detected when the signal enters the probe. This is associated with the impedance mismatch between the probe and the cable. A voltage rise is then observed at *t=18ns* when the signal reaches the end

of the rods (open-ended termination). Finally, multiple reflections occurs until a steady state is attained (not shown in the figure).
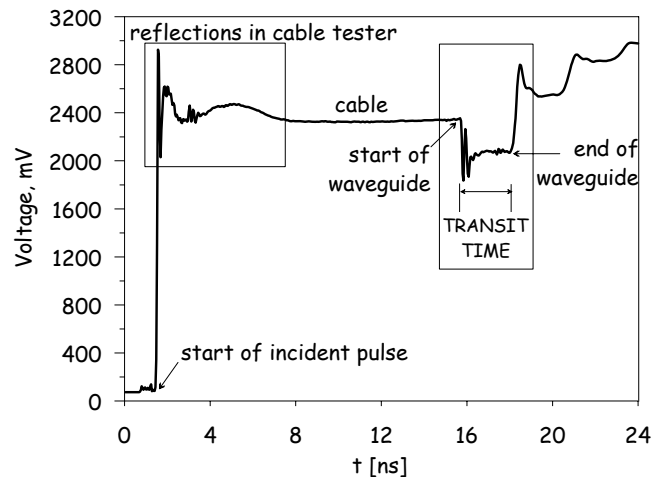

Figure 3. Complete reflection waveform

The time required for the step pulse to travel along the waveguide is used to measure the apparent dielectric permittivity of the soil. The higher is the water content, the higher is the soil bulk permittivity and, hence the lower is the velocity at which the wave propagates into the guide (Robinson *et al.* 2003). The portion of the waveform of interest for travel time determination (box in Figure 3) is shown in Figure 4. In the same figure, the waveforms in air and soil are also shown. The initial dip and the following bump are associated with the transit of the signal through the probe head. The time corresponding to the second ascending limb is associated with signal reflection at the end of the probe (Figure 4).
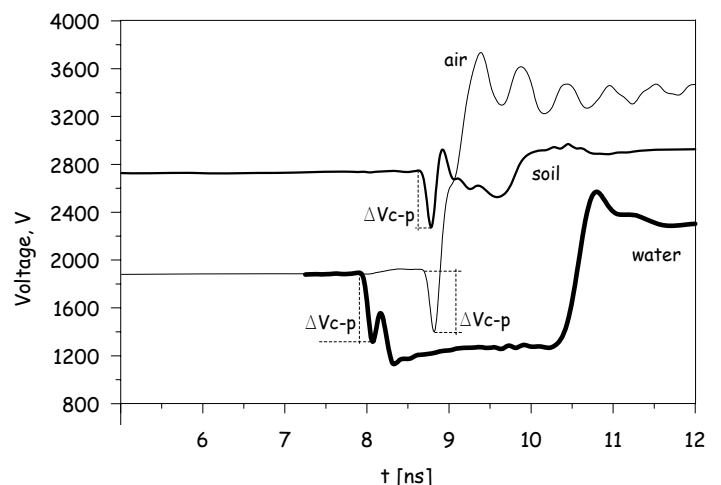

Figure 4. Waveforms in air, water, and soil.

In Figure 4 it can be observed that the waveforms are shifted with respect to time and voltage. This instrument response is surprising. The time at which the signal enters the probe after traveling along the cable should always be the same. Nonetheless, if the waveforms are ideally superposed, one would observe that the first descending limb (valley) is

equal for all waveforms whereas the subsequent first ascending limb (bump) is different. This suggests that the bump cannot be taken as a reference for the beginning of the rods as suggested by other authors (e.g. Or *et al*. 2002). To better understand the nature of the bump located after the first valley of the waveform, a series of measurements was carried out with the probe inserted vertically downward into a low permittivity layer (air) over a high permittivity layer (water). The waveforms collected with the probe sequentially dipped into water are presented in Figure 5.
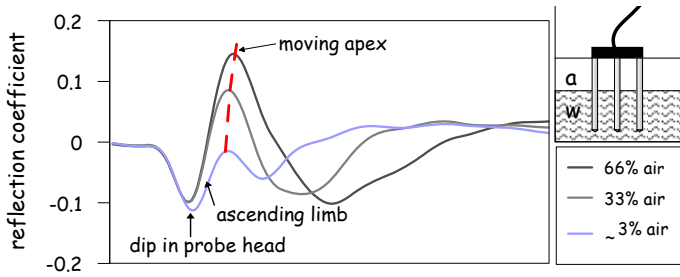

Figure 5. Waveforms measured as the probe is moved from air to water as surrounding medium

The apex of the bump is observed to move forward in time as the probe is removed from water. This confirms that the bump depends on the permittivity of the medium surrounding the rods and it cannot be taken as reference for the beginning of the rods. This has been demonstrated by Robinson *et al*. (2003). A different approach should be therefore developed to identify the beginning of the rods. It would be expected that the beginning of the rods lies somewhere along the first descending limb.

4 WAVEFORM INTERPRETATION

4.1 *Calibration*

The approach suggested by Heimovaara (1993), shown in Figure 6, was used to determine the time at which the signal enters the rods. The signal is represented in term of reflection coefficient, ρ.

The time t_{IN} is the time at which the signal enters the head of the probe. The time t_{FIN}, obtained by the intersection between the line tangent to the second ascending limb is the time at which the signal is reflected at the end of the probe. The time Δt^*, which is the time taken by the signal to travel along the probe head to reach the beginning of the rods, and the effective length of the rods L^* are determined by calibration in air and water. It is assumed that the reflection in water is the slowest, while the reflection in air is the fastest, providing bounds on the possible travel times.

The relationship between the apparent permittivity K_a and the propagation velocity v_P of the signal along the rods can be written as follows:

$$v_P = \frac{L^*}{t_{FIN} - t_{IN} - \Delta t^*} = \frac{c}{\sqrt{K_A}} \qquad (1)$$

where c is the speed of light in vacuum and (t_{FIN}-t_{IN}-Δt^*) determines the value of ΔT. By combining measurements in air (K_a=1) and water (K_a=79.1), the values for Δt^* and L^* equal to 0.136[ns] and 0.0792[m], respectively, were obtained. The time at which the signal enters the rods, ($t_{IN} + \Delta t^*$), was found to be very close to the first waveform valley. We therefore assumed this time could alternatively be taken as reference for the beginning of the rods.
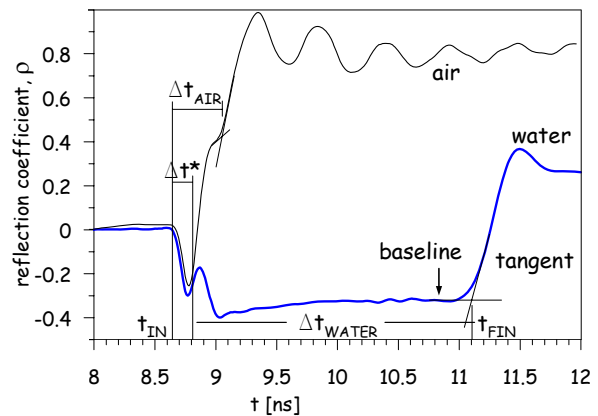

Figure 6. The Heimovaara interpretation of a TDR waveform

4.2 *Waveform interpretation*

Two methods were considered to calculate the transit time from the reflected waveform. In method 1, the time t_{IN} and t_{FIN} were taken as shown in Figure 6, and the apparent permittivity was calculated by considering the values of L^* and Δt^* derived from Eq.(1). In method 2, the length of the rods L^* was assumed to be equal to the physical length (0.08m). In this case, the time Δt^* was set to zero and t_{IN} is taken at the first waveform valley.

5 RESULTS

A comparison between the two procedures used to determine K_a value is shown in the Figure 7. The two methods are essentially equivalent. It may be concluded that, for this TDR system, the time associated with the first waveform valley can be successfully used to identify the beginning of the rods, for cases when TDR measurements in water and air are not available.

The relationship between the apparent permittivity and the volumetric water content for the three series of samples, which are characterized by nominal dry densities of 1.4, 1.5, and 1.7 g/cm^3 respectively, is shown in Figure 8. Topp's equation (Topp *et al*. 1980) is also plotted as a reference (dotted line).

It can be observed that the higher the dry density ρ_d, the higher the apparent permittivity K_a at a given θ_V. This is expected because when ρ is increased, the air ($K_a=1$) is replaced by solids having higher dielectric permittivity ($K_a\sim5$). Overall, all data are located above Topp's equation.
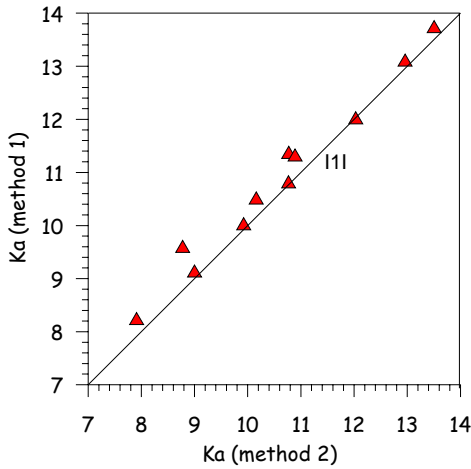

Figure 7. Comparison of the two procedures used to obtain Ka

6 DISCUSSION

To assess the effect of dry density on dielectric permittivity, the three-phase Litchteneker 'refractive index' mixing model was considered:

$$\sqrt{K'}-1=\frac{\rho_{REFd}+\Delta\rho_d}{\rho_s}\left(\sqrt{K_s}-1\right)+\vartheta\left(\sqrt{K_w}-1\right) \quad (2)$$

where K' denotes the real part of the apparent permittivity, K_s and K_w are the permittivity of solids and water, respectively, ρ_s is the density of solids, ρ_{REFd} is a reference bulk dry density and $\Delta\rho_d$ is the variation of dry density with respect to ρ_{REFd}.
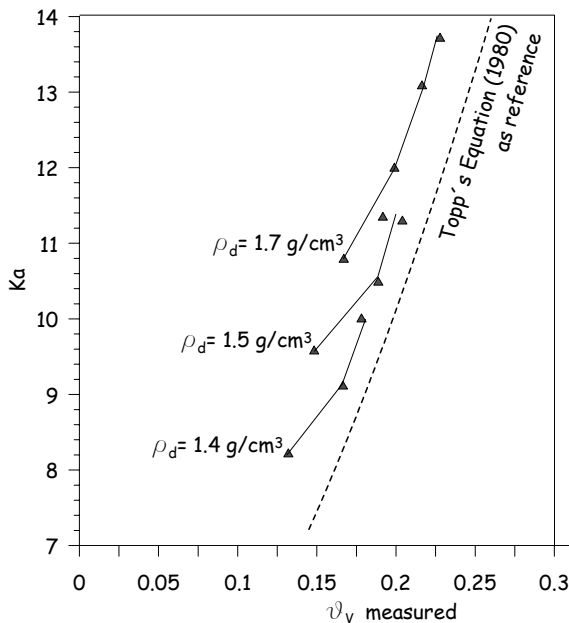

Figure 8. K_a versus θ_v for the three different dry densities (K_a determined using method 1).

The real part of the apparent permittivity K' was used in place of the apparent permittivity K_a to denote the fact that Eq.(2) is written by assuming that the complex part (which reflects the electrical conductivity) is negligible. This model has been found to satisfactorily capture experimental data for the case of soils having low clay content and/or low specific surface (Roth *et al.* 1990; Robinson *et al.* 1999). The Eq.(2) can be written as the follows:

$$\sqrt{K'}=\sqrt{K_{REFd}}+\frac{\Delta\rho}{\rho_s}\left(\sqrt{K_s}-1\right) \quad (3)$$

where K_{REFd} is the permittivity for $\Delta\rho_d=0$. We assumed ρ_{REFd} equal to 1.5g/cm³ because K_{REFd} calculated using Eq.(2) equals K_{TOPP} for this value of ρ_{REFd} (Tarantino *et al.* 2008).
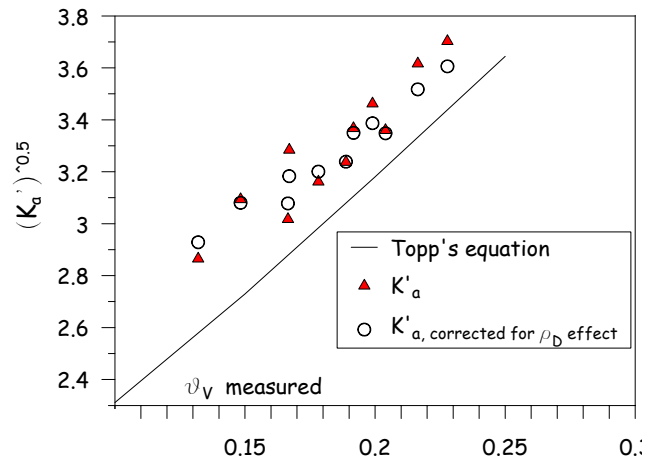

Figure 9. Apparent permittivity K_a data corrected for the effect of dry density

In Figure 9, the measured apparent permittivities corrected by the factor $\Delta\rho(K_s^{0.5}-1)/\rho_s$ are plotted versus the volumetric water content θ_V together with the uncorrected data. It can be observed that corrected data have significant lower dispersion suggesting that the 'refractive index' model adequately captures the effect of dry density.

Nonetheless, data are located above Topp's equation. We checked whether bulk electrical conductivity could explain this discrepancy. In fact, a relative high electrical conductivity tends to increase dielectric permittivity as shown by the equation of apparent permittivity for a sinusoidal plane wave (Von Hippel, 1954):

$$\varepsilon_a=\frac{\varepsilon'}{2}\left(1+\sqrt{1+\left(\left(\varepsilon''_{RELAX}+\sigma/2\pi f_{EFF}\varepsilon_0\right)/\varepsilon'\right)^2}\right) \quad (4)$$

where ε_a is the measured apparent permittivity, ε' and ε'' are the real and imaginary part of the soil dielectric permittivity, respectively, ε_0 the dielectric permittivity in the vacuum, σ is the bulk electrical conductivity and f_{EFF} is the effective frequency in Hz.

The effective frequency f_{EFF} of the signal propagating in water and soil was calculated according to Strickland (1970) as follows:

$$f_{EFF} = \frac{\ln(0.9/0.1)}{2\pi \cdot t_R} \qquad (5)$$

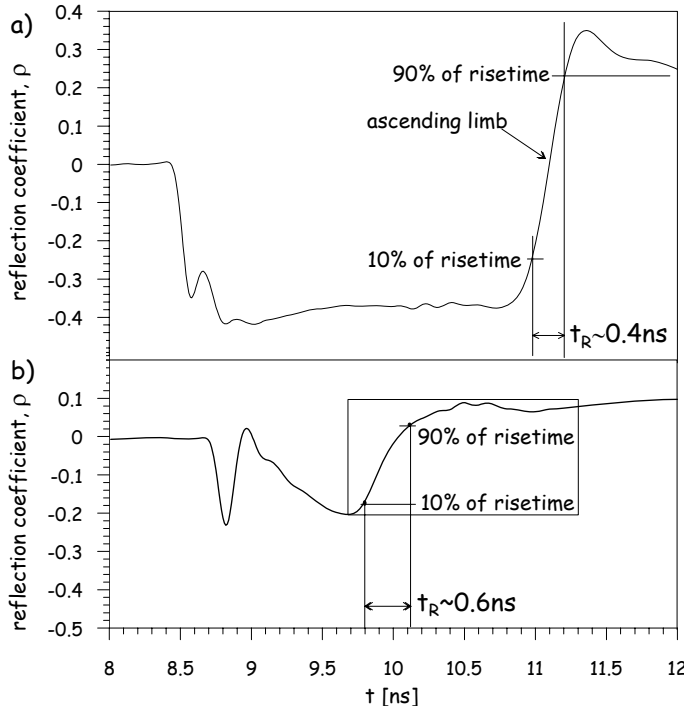where t_R can be obtained according to the construction shown in Figure 10.

Figure 10. Determination of risetime, t_R, from the TDR waveform using the 10%-90% values in water (a) and soil (b)

It was observed that the effective frequency decreases from about 800 MHz to 550 MHz from water to soil respectively. This signal dispersion is due to a non-negligible electrical conductivity. Lower frequency waves are slowed down (see Eq.(4), producing less steep second ascending limb. According to Topp et al. (1988), the bulk electrical conductivity, σ_a, can be calculated from reflection at $t \sim \infty$. Unfortunately, waveforms were recorded by the Trase over a period of time of only 24 ns, which is not enough to measure the reflection coefficient at $t \sim \infty$.

To extrapolate the recorded waveform to higher times, we simulated the waveform according to the approach presented by Lin (2003) for multi-section transmission lines as described by Tarantino and Pozzato (Ibid.). For sake of simplicity, an ideal input function was considered. The specific surface A_s, was estimated from hygroscopic water content according to Dirksen and Dasberg (1993) assuming that a mono-molecular layer of water envelops the clay particles. A value of 67 m²/g was thus obtained.

The measured and simulated waveforms are shown in Figure 11. We tentatively assumed the following values for the permittivity of free water, bound water and solids, ε_{fw}=80.2, ε_{fw}=5, and ε_s=5, respectively, and σ_{fw}=1.1 S/m and σ_{bw}=15 S/m for the electric conductivity of free water and bound water, respectively. The entire simulated waveform was plotted and the value of the reflection coefficient was determined as equal to ~0.2 (Figure 12).
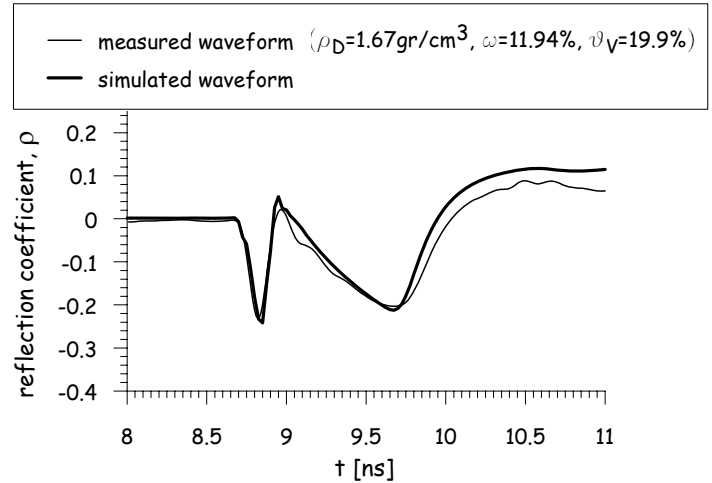

Figure 11. Measured (ρ_s=2.71 g/cm3, ρ_D=1.67 g/cm3, θ_V=0.2) and predicted waveform for soil (A_s=66.7, ε_{fw}=80.2, ε_s=5, σ_{bw}=15 S/m, σ_{fw}=1.1 S/m)

The bulk conductivity, σ_a, was calculated according to Topp et al. (1988):

$$\sigma = \frac{1}{Z_c} \frac{\varepsilon_0 c Z_0}{L} \left[\frac{1-\rho_\infty}{1+\rho_\infty} \right] \equiv \frac{1}{Z_c} \frac{\varepsilon_0 c Z_0}{L} \left[\frac{2V_0}{V_F} - 1 \right] \qquad (6)$$

where ε_0 is the permittivity of free space (8.854·10-12 F m^{-1}), c is the speed of light in a vacuum (3·10^8 m s^{-1}), L is the probe length (0.08m), ρ_∞ the reflection coefficient at infinite time (~0.2), V_0 is the voltage entering the head of the probe, V_F the final voltage recorded by the oscilloscope after all multiple reflections had taken place, Z_c is the characteristic impedance of the cable tester (50Ω), and Z_0 is characteristic impedance of the probe (220Ω). A value of 1dS/m was obtained.
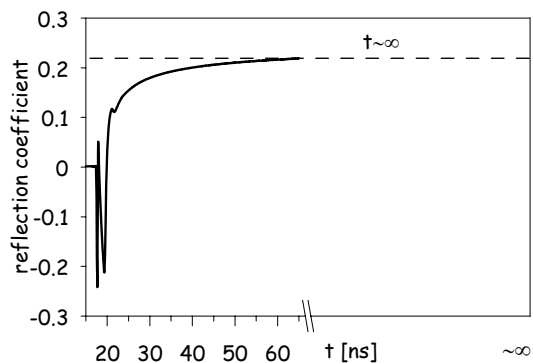

Figure 12. Simulated reflection coefficient from the plotted reflection at t ~ infinite.

To account for the effect of electrical conductivity on apparent permittivity, the empirical approach proposed by Wyseure et al. (1997) was considered:

$$K_a = K' + 1.432\sigma \qquad (7)$$

where σ is the electrical conductivity in dS/m.
If Eq.(7) is substituted in Eq.((3), the following equation is obtained:

$$K_{TOPP} = \left(\sqrt{K_a} - \Delta\rho_d \left(\frac{\sqrt{K_s} - 1}{\rho_s} \right) \right)^2 - 1.432 \cdot \sigma \qquad (8)$$

The values of K_a measured using TDR and the values corrected to account for the combined effect of ρ_d and σ (K_{TOPP} in Eq.(8)) are plotted against volumetric water content θ_V. It can be observed that the corrected data collapse on Topp's calibration curve. This demonstrates again that deviations from Topp's equation occur for dry densities and bulk electrical conductivities outside the range investigated by Topp *et al.* (1980). Nonetheless, simple corrections could be introduced to account for these deviations.
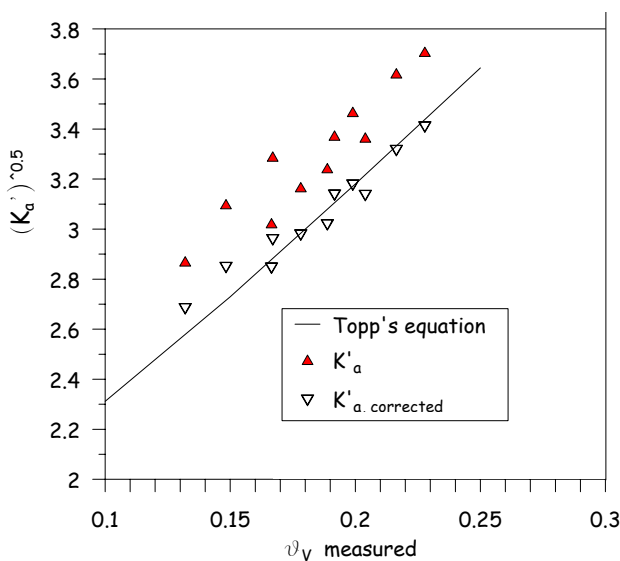

Figure 13. Apparent permittivity Ka as result of the correction in term of dry density and bulk electrical conductivity.

7 CONCLUSIONS

An experimental investigation of the effect of dry density on dielectric apparent permittivity was carry out in this study. It was observed that the effect was not significant, but not negligible for sensitive applications. The effect of dry density was successfully modeled using a three-phase 'refractive index' model. Nonetheless, the measured permittivity corrected for dry density was still underestimated by Topp's equation.
We observed a decrease in effective frequency when measuring the waveform in the soil and we inferred

the soil had non-negligible electrical conductivity. Since the waveform was recorded over a short period of time that was insufficient to reach steady-state conditions, the waveform was simulated to capture the reflection coefficient that would have been recorded at infinite time. This made it possible to estimate the bulk electrical conductivity and to further correct the measured K_a using an empirical equation. Topp's equation was shown to match the corrected data.

REFERENCES

Dirksen C and Dasberg S (1993). Improved calibration of time domain reflectometry soil water content measurements. *Soil Sci. Soc. Am. J.* 57:660–667.
Heimovaara, T.J. 1993. Design of triple-wire time domain reflectometry probes in practice and theory. *Soil Sci. Soc. Am. J.*, 57: 1410-1417.
Lin, C.P. (2003a). Analysis of nonuniform and dispersive time domain reflectometry measurement systems with application to the dielectric spectroscopy of soils. Water Resour. Res. 39
McCartney, J.S. (2007). Determination of the Hydraulic Characteristics of Unsaturated Soils using a Centrifuge Permeameter. *Ph.D. Dissertation*. The University of Texas at Austin.
Or, D., T. VanShaar, J.R, Fisher, R.A. Hubscher, and J.M.Wraith. 2002. *WinTDR99–Users guide*. Utah State University - Plants, Soils & Metereology, Logan, UT.
Robinson DA, Gardner CMK, Cooper JD (1999). Measurement of relative permittivity in sandy soils using TDR, capacitance and theta probes: comparison, including the effects of bulk soil electrical conductivity. *Journal of Hydrology* 223: 198–211
Robinson DA, Schaap M, Jones SB, Friedman SP, and Gardner CMK (2003b). Considerations for Improving the Accuracy of Permittivity Measurement using Time Domain reflectometry : Air-water calibration, effects of cable length. Soil Sci. Soc. Am. J. 67:62–70
Roth K, Schulin R, Flühler H, and Attinger W (1990). Calibration of TDR for water content measurement using a composite dielectric approach . *Water Resources Research*, 26 (10)**: 2267-2273
Strickland J.A. (1970). Time-domain reflectometry measurements. *Tektronix Inc.*, Beaverton, Oregon**: 11-13
Tarantino A., Ridley A.M., and Toll D. (2008). Field measurement of suction, water content and water permeability. *Geotechnical and Geological Engineering,* in press.
Tarantino A. and Pozzato A. (Ibid). Limitations of travel time interpretation of reflection waveform in TDR water content measurement.
Topp GC, Yanuka M, Zebchuk WD, and Zegelin S (1988). Determination of Electrical conductivity using TDR: soil and water esperiments in coaxial lines.. Water Resources Research, 24 (7): 945-952.
Topp, G.C., J.L. Davis, and A.P. Annan. (1980). Electromagnetic determination of soil water content: Measurements in coaxial transmission lines. Water Resour. Res. 16:574–582
Wyseure GCL, Mojid MA and Malik (1997). Measurement of volumetric water content by TDR in saline soils.European. *Journal of Soil Science*, 48: 347-354.